# Local Magnetism and Crystal Fields of Pr in $PrBa_2Cu_3O_7$ Studied by $^{141}Pr$ NMR

K. Nehrke and M. W. Pieper

*Institut für Angewandte Physik, Universität Hamburg, Jungiusstrasse 11, D-20355 Hamburg, Germany*

(Received 27 October 1995)

We present the first study of the $^{141}Pr$ nuclear resonance in $PrBa_2Cu_3O_7$. In strong contrast to the current understanding of $PrBa_2Cu_3O_7$, we observe a small ordered Pr moment at low temperatures ($0.017\mu_B$), oriented perpendicular to the $c$ axis, and a temperature and field independent Van Vleck susceptibility below 10 K. We find a $\Gamma_1$ ground state symmetry and a larger splitting of the quasitriplet than observed in inelastic neutron scattering. We propose that the origin of the $(\frac{1}{2}, \frac{1}{2}, 0)$ Bragg peak in neutron diffraction is a ferromagnetic coupling between the $CuO_2$ planes of a bilayer induced by Pr.

PACS numbers: 75.25.+z, 75.10.Dg, 76.60.Lz

One of the outstanding problems in the high-$T_c$ superconducting cuprates $REBa_2Cu_3O_7$ is the supression of superconductivity by Pr on the rare earth (RE) site. In the past years a general consensus has been reached on the basis of photoemission [1,2] and inelastic neutron scattering (INS) studies [3,4] that the valence of Pr is predominantly $3+$ and that holes are doped into the $CuO_2$ layer when filling the chains with oxygen. Pr localizes these holes, probably due to hybridization of the $4f$ and the antibonding $O_{2p\pi}$ orbitals, as proposed by Fehrenbacher and Rice [5].

The local electronic properties were investigated, among others [6], in various NMR studies of the Cu(1) (chain), Cu(2) (plane) [7–10], and O sites [11]. The electric field gradients at the Cu(1) sites are, for all oxygen coordinations, almost identical to the corresponding ones in other $REBa_2Cu_3O_7$ cuprates. Even in the presence of the hole states the quadrupole splitting and magnetic hyperfine field at the Cu(2) site are also similar to the antiferromagnetic reduced compounds, indicating that the Cu moment and its orientation in the plane are unchanged, and that the holes are probably not localized at the Cu site. This is supported by the observation that only the nuclear resonance of one oxygen site in the plane is affected by the presence of Pr [11].

Despite the general consensus on the valence and the crystal field (CF) of Pr, and although the magnetic susceptibility has been fitted by the single ion contributions of $Pr^{3+}$ in this CF [3], there are a number of open problems in the description of the low-temperature magnetic response of Pr. One is the high Néel temperature of $T_N = 12$ to 18 K, depending on the oxygen concentration. This is 8 times the value for Gd in the same structure [12], although the $^3H_4$ multiplet of $Pr^{3+}$ has a nonmagnetic singlet ground state in the orthorhombic coordination. From this point of view the ordered Pr moment of $0.7\mu_B$ observed in neutron diffraction [13] is also surprisingly large. It is an order of magnitude larger than that in the tetragonal site symmetry in the related cuprate $Pr_2CuO_4$, where a smaller crystal field splitting of the low lying eigenstates and thereby a higher induced magnetic moment might be expected [14]. We note, in addition, that the current description of the homogeneous susceptibility neglects the magnetic phase transition of the Pr moments as well as any contribution from the $CuO_2$ sublattice despite the comparably large Pr moment and the rather complicated magnetic phase diagram of the $CuO_2$ planes below 20 K found in a recent neutron diffraction work [15].

Clearly it is very desirable to investigate the $^{141}Pr$ resonance, which provided detailed information on the valence, the local susceptibility, and low-energy crystal field splittings of Pr in $Pr_{1.85}Ce_{0.25}CuO_4$ [16]. In the following, we present the first study of the Pr spin echo in $PrBa_2Cu_3O_7$ and discuss the implications of our results for the interpretation of the homogeneous susceptibility, neutron diffraction, and inelastic neutron scattering.

The home-made phase coherent pulse spectrometer and the samples used in this work are the same as described in a previous work on the NMR and NQR of Cu(1) and Cu(2) sites in $PrBa_2Cu_3O_6$ and $PrBa_2Cu_3O_7$ [7].

Figure 1 shows field-sweep spectra at different fixed frequencies and 1.3 K. With the field $B_0$ along $a = (100)$ or $b = (010)$, which cannot be distinguished in the twinned crystal, we find a nearly resolved splitting of the line below $\approx$2.5 T. The effective gyromagnetic ratio is anisotropic, approaching $\frac{\gamma_a}{2\pi} = 72$ MHz/T and $\frac{\gamma_b}{2\pi} = 67$ MHz/T in high field. Because of the twinning, the assignment to the axes is arbitrary. In a field along the $c$ axis the effective gyromagnetic ratio drops to $\frac{\gamma_c}{2\pi} = 19.5$ MHz/T, and no splitting is observed in low external fields. Extrapolating to zero field we were able to observe the zero-field resonance above 25 MHz (inset). The zero-field spectrum continues to lower frequency, but is difficult to separate from the Cu(1) signal, and below 20 MHz the spin-spin relaxation time $T_2$ is too small to obtain a reliable spectrum in our spectrometer. In Fig. 1 we also show that within the experimental resolution there is no change of $\gamma_c$ between 1.3 and 8 K at high fields. Finally, a comparison of two spectra taken at 79 MHz with field along (100) and (110) shows that the splitting also disappears when the field is applied along a (110) direction.

 0031-9007/96/76(11)/1936(4)$10.00 

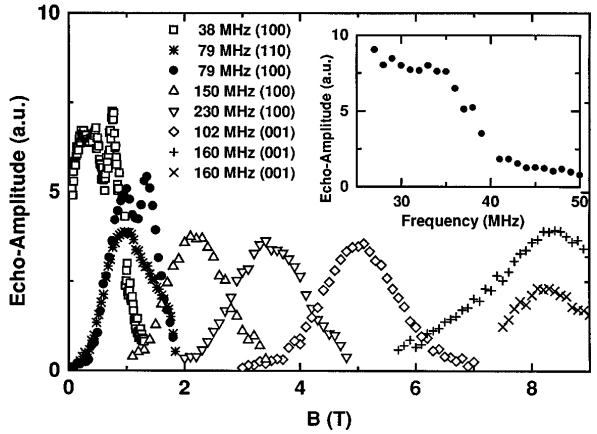


FIG. 1. Field-sweep spectra of $^{141}$Pr in $PrBa_2Cu_3O_7$ at 1.3 K for frequency and orientation of the field as given in the figure. Fields applied along (100) are due to the twinning also along (010). The spectrum at high field is also shown for $T = 8$ K ($\times$). The inset shows the part of the zero-field spectrum we could measure.

Both the spin-lattice and spin-spin relaxation time $T_1$ and $T_2$ increase steeply with external field from 50 and 6 $\mu$s at zero field to 800 and 30 $\mu$s, respectively, at 8 T. At this field, $T_1$ and $T_2$ decrease with increasing temperatures to 80 and 12 $\mu$s, respectively, at 4.2 K.

The signal is not due to other phases containing Pr, since we observed the same signal with the expected broadening from the anisotropy also in independently prepared ceramics. In addition, the signal is larger than the Cu(2) echo for optimum excitation conditions near $B_0 = 6.0$ T ($B_0 \| c$), where the frequency is comparable to the Cu(2) zero-field NMR. Most probably the signal has not been reported up to now because of the small $T_2$ in zero field and the inhomogeneous broadening of powder spectra in external field. In addition, we note the large enhancement factor for the rf field: The pulse power used for measuring the spectra in Fig. 1 is $\sim$20 dB below the optimum for the Cu(2) resonance.

The Pr signal overlaps with the known Cu(1) and Cu(2) spectra in certain field regimes but is unambiguously identified by the effective high-field gyromagnetic ratios, which are 2 to 6 times larger than the ones of the Cu isotopes. The gyromagnetic ratio of the free Pr ion ($\frac{^{141}\gamma}{2\pi} = 13.0$ MHz/T) is also smaller, but giant, anisotropic paramagnetic shifts due to the Van Vleck susceptibility are a well known feature of RE ions with singlet ground states.

We write the total electronic and nuclear spin Hamiltonian in the form

$$H = H_{\rm cf} + g_J \mu_B \mathbf{J}\mathbf{B}_0 + A_J \mathbf{J}\mathbf{I} - {}^{141}\gamma\hbar\mathbf{I}\mathbf{B}_0 . \qquad (1)$$

$H_{\rm cf}$ is the crystal-field Hamiltonian of the $4f$ shell, $g_J = 0.8$ is the Landé factor of the $^3H_4$ configuration of $Pr^{3+}$ according to Hund's rules, $\mu_B$ is Bohr's magneton, $\mathbf{J}, \mathbf{I}$ are the operators of the total electronic angular momentum and the nuclear spin, $\mathbf{B}_0$ is the external field, and $A_J/h = 1093$ MHz [16] is the hyperfine coupling constant of $Pr^{3+}$.

The effective gyromagnetic ratio follows from the electronic magnetization by straightforward substitution of $\mathbf{J}$ in the nuclear part of the spin Hamiltonian Eq. (1) by its expectation value,

$$H_N = -\left(\frac{A_J\langle\mathbf{M}\rangle}{g_J\mu_B} + {}^{141}\gamma\hbar\mathbf{B}_0\right)\mathbf{I} . \qquad (2)$$

$\langle\mathbf{M}\rangle$ and $\mathbf{B}_0$ are parallel when the field is applied along the principal axes $\alpha = a, b, c$. The equidistant splitting of the nuclear energy levels is ascribed to an effective nuclear gyromagnetic constant $\gamma_\alpha$,

$$\frac{\gamma_\alpha}{2\pi} = \frac{\nu}{B_{0,\alpha}} = \frac{A_J}{h}\frac{\langle M_\alpha\rangle}{g_J\mu_B}\frac{1}{B_{0,\alpha}} + \frac{^{141}\gamma}{2\pi} . \qquad (3)$$

The experimental finding of a linear field dependence of $\nu$ on the field in all principal directions at 1.3 K (Fig. 2) then implies that $\langle M\rangle$ is proportional to $B_0$, or that the Van Vleck susceptibility is independent of the field. The measurement at 8.3 K shows that the variation with temperature is also smaller than 1%, at least in a field of $\sim$8 T. Both observations are incompatible with the Kramers doublet ground state of $Pr^{4+}$ and clear evidence for $Pr^{3+}$, confirming the results of photoemission [1,2] and INS [3,4]. The presence of a major amount of $Pr^{4+}$ is in view of the large $Pr^{3+}$ signal intensity improbable, but our failure to detect $Pr^{4+}$ clearly does not exclude its presence.

We can determine the size of the Pr moments in high field from the experimental $\gamma_\alpha$ and Eq. (3). We find for the Pr moment induced by a field of 1 T $\langle M_\alpha\rangle = 0.043\mu_B, 0.040\mu_B$, and $0.0048\mu_B$ for $\alpha = a, b, c$, with an error well below 10%. The assignment to the $a$ and $b$ axes is arbitrary, due to the twinning of the crystal. In zero field the resonance frequency of 23 MHz

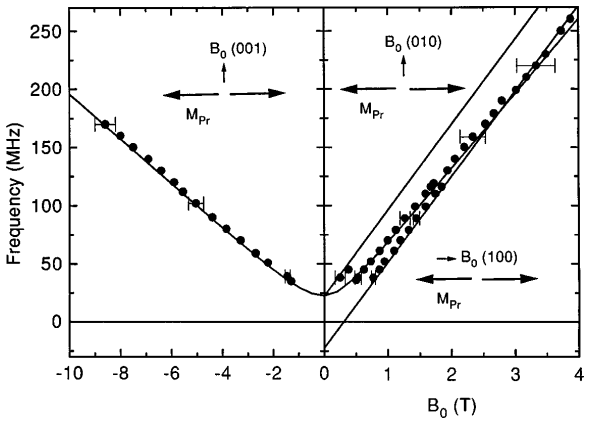


FIG. 2. Field dependence of the $^{141}$Pr-resonance frequency at 1.3 K with the field along (001) (left) and (100), (010) (right). The lines are calculated from Eq. (3) with the magnetization according to the crystal-field parameters in Table I.

corresponds directly to a static moment of $g_J h\nu/A_J = 0.017\mu_B/\mathrm{Pr}$, smaller than the one in $Pr_2CuO_4$.

Such a small Pr moment is in clear contrast to the current interpretation of the large magnetic Bragg peaks observed in neutron diffraction below 18 K in $PrBa_2Cu_3O_7$ [13]. A moment of $0.017\mu_B$ corresponds to nearly undetectable small Bragg reflections. We emphasize, therefore, that the evidence for the small moment presented here is quite strong, once the applicability of Hund's rules for $Pr^{3+}$ is accepted: There are no free parameters except the magnetic moment in Eq. (3), which describes the full field and orientation dependence of the Pr NMR at low temperatures (full lines in Fig. 2, see below).

We conclude that the large magnetic Bragg peaks observed in $PrBa_2Cu_3O_7$ at low temperatures originate from the CuO sublattices. The NQR of the Cu(1) sites excludes the presence of any sizable static moment in the chains of our Al-free crystal [7]. The magnetic response of the $CuO_2$ planes is a difficult problem. On one hand, we cannot exclude that the localized holes in the planes might carry a moment [4]. The moments would have to be localized at the oxygen, because the NMR spectrum of Cu in the plane is very similar to the one in the $REBa_2Cu_3O_6$ cuprates. We believe it is very improbable that ordering of the small Pr moments induces magnetic order in such hole states, which should then account for the Bragg peak. On the other hand, it has been noted in recent neutron diffraction work that for Al-doped crystals the magnetic transition of the Cu bilayers from the so-called antiferromagnetic AF-I to the AF-II structure gives rise to Bragg peaks at $(\frac{1}{2}, \frac{1}{2}, \frac{1}{2})$, also assigned to Pr [10,15]. Antiferromagnetically coupled Cu bilayers still cannot contribute to the main magnetic peak $(\frac{1}{2}, \frac{1}{2}, 0)$, due to a vanishing form factor. We propose that Pr couples the two adjacent $CuO_2$ layers below 18 K ferromagnetically. In this way it may induce a ferromagnetic stacking sequence of the $CuO_2$ planes. The small Pr moment is, in this model, a consequence of the dipolar field from the Cu moments ($B_{\mathrm{dip}} \approx 0.15$ T) and Pr exchange fields. The transferred hyperfine fields present in $Pr_2CuO_4$ [14] vanish by site symmetry. No critical behavior has been detected in the Cu(1) NQR up to 20 K, so the rearrangement of Cu(2) spins must occur in a noncritical manner.

The induced Pr moment must be oriented along the dipolar field, which is perpendicular to the $c$ axis. The presence of a single line when the field is applied along the $c$ axis shows that the ordered Pr moments are indeed within $\pm 15^\circ$ perpendicular to the $c$ axis. Otherwise, the corresponding component of the hyperfine field in the two antiferromagnetic sublattices would add or subtract from the external field (insets to Fig. 2), leading to a broadening or splitting. The splitting with field applied along (100) and (010) into three broad peaks is due to the vector addition of the external and the transferred field inducing the moment (see Fig. 2). The spontaneous moments are aligned along either (100) or (010), because no splitting of the line can be resolved with the field along (110) (Fig. 1). This orientation of the Pr moments is in contrast to the one proposed tentatively from neutron scattering [3] but in agreement with Mössbauer experiments [17] and our analysis of the Cu NMR and NQR in $PrBa_2Cu_3O_6$.

In order to discuss the field dependence of the resonance frequency (Fig. 2) and to determine the crystal-field splittings from the field-induced Pr moments, we neglect the small influence of the nuclear contributions to the electronic magnetization and calculate the expectation value of $\mathbf{M}$ by a numerical diagonalization of the electronic part $H_{\mathrm{el}}$ without the two nuclear contributions,

$$H_{\mathrm{el}} = g_J \mu_B \mathbf{J}\mathbf{B}_0 + \sum_{l=1}^{6} \sum_{m=0}^{l} B_{lm} O_l^m ,$$
$$\langle \mathbf{M} \rangle = \frac{-g_J \mu_B \mathrm{Tr}\{\exp(-H_{\mathrm{el}}/k_B T)\mathbf{J}\}}{\mathrm{Tr}\{\exp(-H_{\mathrm{el}}/k_B T)\}} . \quad (4)$$

We measured only at low temperatures and neglect the admixture of multiplets with higher angular momentum ($J = 5, 6$) observed in INS. Within the nine energy levels of the multiplet $J = 4$, we can use standard Steven's operators $O_l^m$ for the $4f$ shell [18]. Only operators compatible with the transformations of the Pr site symmetry ($2/mm$ or $D_{2h}$) contribute, namely, $l = 2, 4, 6$, $m = 0, 2, 4, 6 \leq l$. Our data are clearly insufficient to determine independently the nine crystal-field parameters $B_{lm}$ of $H_{\mathrm{cf}}$ in orthorhombic symmetry without further information, thus we also fit the upper six crystal-field energies observed in INS [3].

The anisotropic susceptibility is dominated by the large matrix elements $\langle \Psi_0 | J_{x,y} | \Psi_{1,2} \rangle$ (in plane) and $\langle \Psi_0 | J_z | \Psi_3 \rangle$ (parallel $c$) and determines $E_0, \ldots, E_3$ in Table I to within $\approx 10\%$ and the $\Gamma_1$ symmetry of the ground state. The best fit to the energies and our high field data was obtained with $B_{20}$ and $B_{22}$ to describe the orthorhombic distortion: $B_{40} = 0.325$, $B_{44} = 1.665$, $B_{60} = -0.0022$, $B_{64} = 0.0252$, $B_{20} = -1.9$, and $B_{22} = 1.2$ (in kelvin). The errors are large since $B_{42}$, $B_{62}$, and $B_{66}$ can be introduced as well to describe the orthorhombicity; the present choice is mainly for convenience. The $B_{lm}$ given here should guide a possible reevaluation of the INS data, including the $\Gamma_1$ ground state symmetry and the larger splitting of the quasitriplet. In order to describe the deviations from straight lines at low field in Fig. 2 in the present approximation we introduce a local magnetic field by $B_{11} O_1^1$ and fitted the full experimental field dependence of the Pr resonance (lines in Fig. 2) with $B_{11} = 0.2$ K, corresponding to 0.38 T, and an orthorhombic distortion $B_{42} = -0.08$ K instead of $B_{22}$. The field is only a factor of 2 larger than the pure dipolar field from the nearest Cu neighbors in the arrangement proposed above. This set of $B_{lm}$ fits our magnetization data, the transition energies observed in INS, and the susceptibility $\chi$. Below 20 K we calculate $\chi_{xx} = 3.0 \times 10^{-3}$,

TABLE I. Eigenvalues $E_i$ and eigenstates of $H_{\mathrm{cf}}$ for the fit to the high field $\gamma$ without molecular field. The lines in Fig. 2 were calculated with a transferred field, $B_{11} = 0.2$ K, and with $B_{42} = -0.08$ K instead of $B_{22}$, which gives nearly the same energies. The sign $\pm$ in $\Psi_i$ denotes a sum of both values ($\Psi_0 = 0.01|4\rangle - 0.01|-4\rangle + 0.71|-2\rangle - 0.71|2\rangle$).

| $i$ | $E_i$ (K) | $\Psi_i = \sum_{m=-4}^{4} a_m\|m\rangle$ |
|---|---|---|
| 0 | 0 | $\pm 0.01\|\pm 4\rangle \pm 0.71\|\mp 2\rangle$ |
| 1 | 132 | $0.66\|\pm 3\rangle - 0.26\|\pm 1\rangle$ |
| 2 | 142 | $\pm 0.66\|\pm 3\rangle \pm 0.26\|\pm 1\rangle$ |
| 3 | 726 | $0.71\|\pm 2\rangle - 0.05\|0\rangle$ |
| 4 | 775 | $0.65\|\pm 4\rangle - 0.01\|\pm 2\rangle - 0.4\|0\rangle$ |
| 5 | 832 | $\pm 0.71\|\pm 4\rangle \pm 0.01\|\pm 2\rangle$ |
| 6 | 922 | $\pm 0.26\|\pm 3\rangle \pm 0.66\|\mp 1\rangle$ |
| 7 | 956 | $0.26\|\pm 3\rangle + 0.66\|1\rangle$ |
| 8 | 1126 | $0.29\|\pm 4\rangle + 0.03\|\pm 2\rangle + 0.91\|0\rangle$ |

$\chi_{yy} = 2.55 \times 10^{-3}$, and $\chi_{zz} = 0.2 \times 10^{-3}$, independent of the temperature. The isotropic mean value $\chi_{\mathrm{iso}}$ falls above 20 K roughly according to a Curie law. This accounts for $\approx 50\%$ of $\chi_{\mathrm{iso}}$ observed in powders and ceramics [3,19], as well as the constant effective $\gamma$ below 10 K in our experiment.

In conclusion, the $^{141}$Pr NMR data presented here show that the static moment of Pr in $PrBa_2Cu_3O_7$ at low temperatures is only $0.017\mu_B$, 40 times smaller than the value deduced from neutron diffraction. The easy axis of the moment is along (100) or (010). The effective gyromagnetic ratio of $^{141}$Pr is anisotropically enhanced by the Van Vleck susceptibility. Our analysis of the crystal field parameters is in general accord with the homogeneous susceptibility above 20 K and models based on inelastic neutron scattering, but we find a larger splitting of the low lying quasitriplet with a smaller orthorhombic distortion and a $\Gamma_1$ ground state symmetry. This leads to a larger susceptibility in the $a$-$b$ plane than along the $c$ axis, as observed in our resonance data. We propose that the magnetic Bragg peaks observed in neutron diffraction below 18 K are due to a change of the stacking of the $CuO_2$ layers induced by a ferromagnetic coupling between the two layers adjacent to Pr.

We had many interesting discussions with Professor J. Appel and Dr. H. Lütgemeier. Professor J. Kötzler kindly supported the work at his institute in Hamburg. It is a pleasure to give our thanks to T. Wolf who prepared the beautiful crystal. K. N. acknowledges support by a grant from the University of Hamburg. The work was supported by the Deutsche Forschungsgemeinschaft.

[1] J. Fink, N. Nücker, H. Romberg, M. Alexander, M. B. Maple, J. J. Neumeier, and J. W. Allen, Phys. Rev. B **42**, 4823 (1990).
[2] D. D. Sarma, P. Sen, R. Cimino, C. Carbope, W. Gudat, E. V. Sampathkumaran, and I. Das, Solid State Commun. **77**, 377 (1991).
[3] G. Hilscher, E. Holland-Moritz, T. Holubar, H.-D. Jostarndt, V. Nekvasil, G. Schaudy, U. Walter, and G. Fillion, Phys. Rev. B **49**, 535 (1994), and references therein.
[4] K. Kodama, S. Shamoto, H. Harashina, M. Sato, M. Nishi, and K. Kakurai, J. Phys. Soc. Jpn. **63**, 4521 (1994).
[5] R. Fehrenbacher and T. M. Rice, Phys. Rev. Lett. **70**, 3471 (1993).
[6] H. B. Radousky, J. Mater. Res. **7**, 1917 (1992).
[7] K. Nehrke, M. W. Pieper, and T. Wolf, Phys. Rev. B **53**, 1 (1996).
[8] K. Yoshimura, N. Saga, T. Sawamura, M. Kato, T. Shimizu, and K. Kosuge, Physica (Amsterdam) **235C-240C**, 1701 (1994).
[9] A. P. Reyes, D. E. MacLaughlin, M. Takigawa, P. C. Hammel, R. H. Heffner, J. D. Thompson, and J. E. Crow, Phys. Rev. B **43**, 2989 (1991).
[10] H. Lütgemeier and I. Heinmaa, in *Proceedings of the 26th Zakopane Summer School on Physics* (World Scientific, Singapore, 1991), p. 264.
[11] Y. H. Ko, H. K. Kweon, H. C. Lee, and N. H. Hur, Physica (Amsterdam) **224C**, 357 (1994).
[12] B. W. Lee, J. M. Ferreira, Y. Dalichaouch, M. S. Torikachvili, K. N. Yang, and M. B. Maple, Phys. Rev. B **37**, 2368 (1988).
[13] W.-H. Li, J. W. Lynn, S. Skanthakumar, T. W. Clinton, A. Kebede, C.-S. Jee, J. E. Crow, and T. Mihalisin, Phys. Rev. B **40**, 5300 (1989).
[14] M. Matsuda, K. Yamada, K. Kakurai, H. Kadowaki, T. R. Thurston, Y. Endoh, Y. Hidaka, R. J. Birgenau, P. M. Gehring, A. H. Moudden, and G. Shirane, Phys. Rev. B **42**, 10 098 (1990).
[15] A. Longmore, A. T. Boothroyd, C. Changkang, H. Yongle, M. P. Nutley, N. H. Andersen, H. Casalta, P. Schleger, and A. N. Christensen, Phys. Rev. B (to be published).
[16] O. N. Bakharev, A. G. Volodin, A. V. Duglav, A. V. Egorov, M. V. Eremin, A. Yu. Zavidonov, O. V. Lavizina, M. S. Tagirov, and M. A. Teplov, Sov. Phys. JETP **74**, 370 (1992).
[17] J. A. Hodges, G. le Bras, P. Bonville, P. Imbert, and G. Jehanno, Physica (Amsterdam) **218C**, 283 (1993).
[18] M. T. Hutchings, in *Solid State Physics*, edited by F. Seitz and D. Turnbull (Academic Press, New York, 1964), Vol. 16, p. 254.
[19] A. Kebede, C. S. Jee, J. Schwegler, J. E. Crow, T. Mihalisin, G. H. Myer, R. E. Salomon, P. Schlottmann, M. V. Kuric, S. H. Bloom, and R. P. Guertin, Phys. Rev. B **40**, 4453 (1989).